



Fermi National Accelerator Laboratory

FERMILAB-Conf-95/239-E

CDF

Physics Prospects with the Upgraded CDF Detector

J. Huyen

For the CDF Collaboration

*Fermi National Accelerator Laboratory
P.O. Box 500, Batavia, Illinois 60510*

July 1995

Published Proceedings for the *10th Topical Workshop on Proton-Antiproton Collider Physics*,
Fermi National Accelerator Laboratory, Batavia, Illinois, May 9-13, 1995

Disclaimer

This report was prepared as an account of work sponsored by an agency of the United States Government. Neither the United States Government nor any agency thereof, nor any of their employees, makes any warranty, expressed or implied, or assumes any legal liability or responsibility for the accuracy, completeness, or usefulness of any information, apparatus, product, or process disclosed, or represents that its use would not infringe privately owned rights. Reference herein to any specific commercial product, process, or service by trade name, trademark, manufacturer, or otherwise, does not necessarily constitute or imply its endorsement, recommendation, or favoring by the United States Government or any agency thereof. The views and opinions of authors expressed herein do not necessarily state or reflect those of the United States Government or any agency thereof.

Physics prospects with the upgraded CDF detector

Jim Hlyen
Fermilab (CDF Collaboration)

The CDF detector is being extensively upgraded for Fermilab Tevatron Run II, which is scheduled to begin in 1999. This talk describes the planned detector upgrades. The power of the upgraded detector is illustrated by showing the expected precision of several physics measurements that will be made with the Run II data: the top mass, the W mass, $\text{BR}(t \rightarrow Wb)$, and the CP violation parameters $\sin(2\alpha)$ and $\sin(2\beta)$.

The next Tevatron run (Run II) is expected to produce luminosities $> 10^{32} \text{cm}^{-2} \text{sec}^{-1}$, compared to the current $2 \times 10^{32} \text{cm}^{-2} \text{sec}^{-1}$, allowing substantially larger data sets to be accumulated. Several upgrades to the CDF detector will be necessary to handle the increased event rate. In addition, important new capabilities will be added to the CDF detector, that will extend the physics reach beyond just a simple scaling of the luminosity. The combination of the upgraded Tevatron and the upgraded detector will enable a very large array of physics measurements to be made with the CDF detector in Run II. For the top quark, this includes improved measurement of the top mass, top production mechanisms, and top decay channels. Electro-weak measurements include the W mass, di-boson production, W production asymmetry, and demonstration of the $W\gamma$ radiation zero. In the b quark system, CDF will be able to measure CP violation, rare decays, mixing parameters, masses and lifetimes. An indirect measurement of the Higgs mass will be possible using the top and W mass measurements, and a direct search for Higgs from top decay can be made. In the exotic sector, searches will be made for leptoquarks, excited quarks, axiguons, etc. QCD measurements include parton distribution functions, α_s , and jets plus W , Z .

TABLE 1. Upgrade of the silicon vertex detector.

Detector Parameter	SVX'	SVX II
Readout coordinates	$r - \phi$	$r - \phi, r - z$
Number of layers	4	5
Total length	51 cm	96 cm
$r - \phi$ readout channel length	25.5 cm	16 cm
Inner radius	3.0 cm	2.4 cm
Outer radius	7.8 cm	10.7 cm
$r - \phi$ readout pitch	60;60;60;55	60;62;60;60;57
$r - z$ readout pitch	-	150;133;60;150;57
$r - \phi; r - z$ readout channels	46,080; 0	221,184; 202,752

THE CDF DETECTOR UPGRADES

Figure 1 shows the current CDF detector configuration for Run I, and the upgraded configuration for Run II. Figure 2 shows a blow up of the tracking volume and endplug calorimeter for Run II. Each of the detector upgrades will be addressed below, beginning with the innermost elements.

SVX II

The Silicon Vertex Detector (SVX) is used for detecting the rather small track impact parameters induced by the decay path length of beauty and charm hadrons.

The new silicon strip vertex detector (SVX II) will contain several major improvements over the current SVX' detector (Table 1). SVX II will be nearly twice as long as SVX', improving acceptance; SVX II will use the back side of the silicon detectors to obtain stereo measurements of track positions, and thus will measure the impact parameter of tracks in the $r - z$ view as well as the $r - \phi$ view; and SVX II will have one more layer than SVX'. As shown in Figure 3, there will be three layers of 90 degree stereo, used to give good impact parameter resolution, and two layers of small angle stereo, used to do associate the $r - z$ and $r - \phi$ views of tracks. Figure 4 shows the calculated impact parameter resolution, which in the upgraded system will be quite good even out to pseudo-rapidity of 2.

Intermediate Fiber Tracker (IFT)

A set of cylindrical scintillating fiber layers (Figure 5) will be installed at a radius intermediate between the SVX II and the main Central Tracking Chamber (CTC) ¹. The IFT will be built from 54,000 channels of 0.5 mm

¹Since the function of measuring the vertex z position will be taken over by the SVX II, the gas wire chamber which currently serves that function (the VTX) can

CDF Detector Evolution

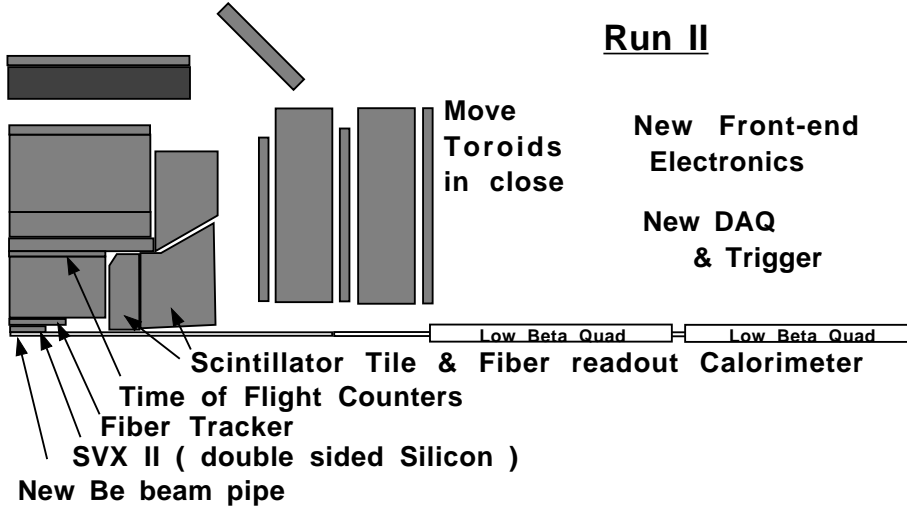
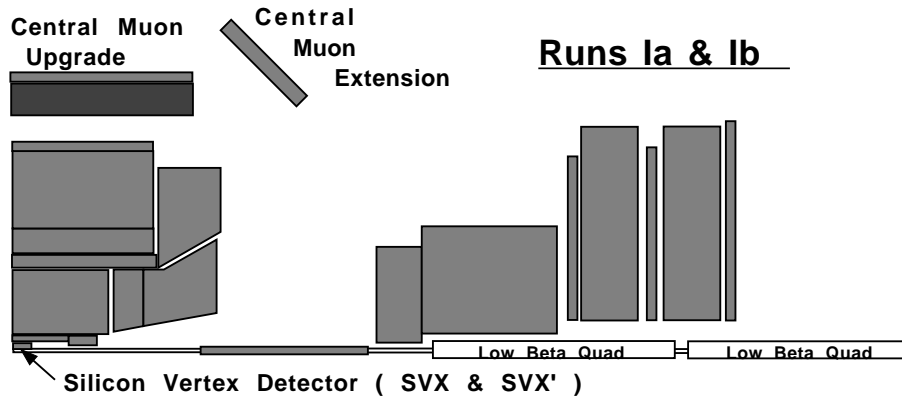
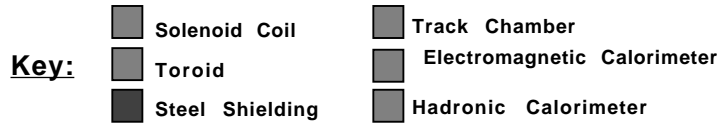


FIG. 1. The CDF detector in its current Run I configuration, and as upgraded for Run II.

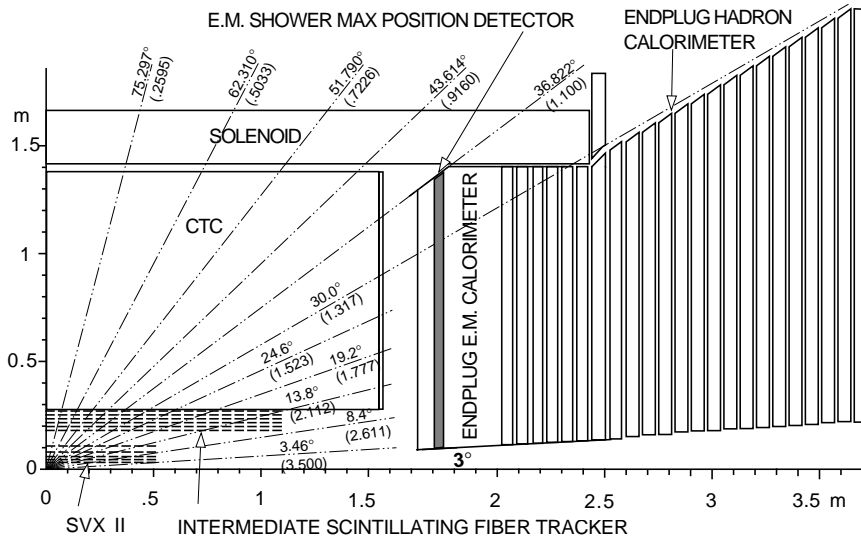


FIG. 2. The CDF detector tracking volume and endplug calorimeter for Run II. The dot-dashed lines show polar angle and pseudorapidity.

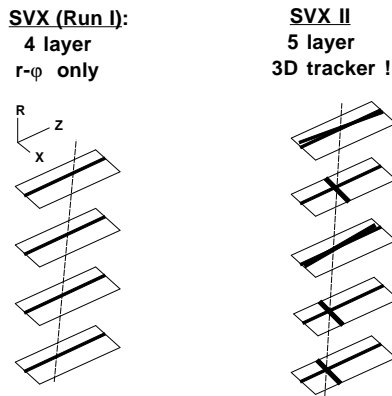


FIG. 3. Cartoon of hits produced by a track in the SVX II compared to the SVX. The double sided readout from the SVX II detectors produces stereo as well as axial information.

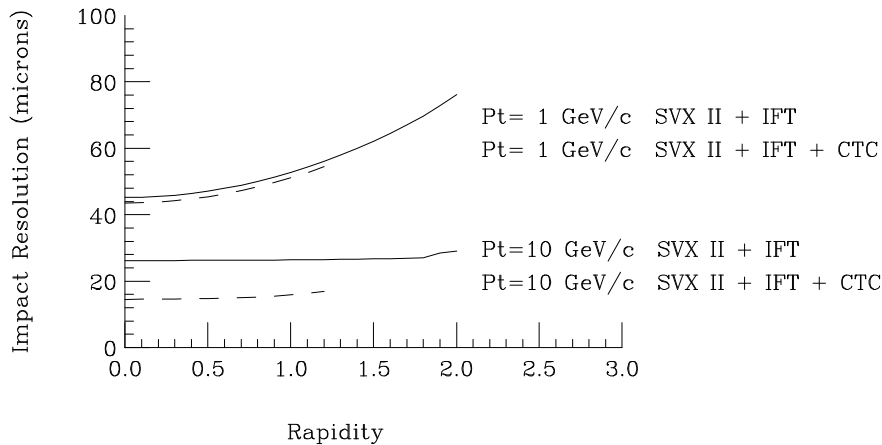


FIG. 4. Calculated impact parameter resolution in the $r - \phi$ plane of the SVX II in combination with the IFT, and in combination with the entire tracking system.

diameter scintillating fiber connected by clear fiber to VLPC photon detectors. It is designed to give 6 axial and 6 small angle stereo measurements on each track, with a resolution of ~ 100 microns per layer. The motivation is twofold.

- The IFT combined with the SVX II will provide robust tracking for pseudo-rapidities out to $|\eta| \sim 2$. This coverage matches the longer SVX II coverage; it is well past the fiducial area of the CTC (see Figure 4).
- The IFT will work as an inner superlayer in combination with the outer tracker for tracking applications which require the momentum precision of the full tracking volume. This extends the luminosity reach of the current CTC, where as the luminosity approaches $10^{32} \text{cm}^{-2} \text{sec}^{-1}$, the inner layers of the CTC are overwhelmed by occupancy. With an eventual CTC replacement, the fiber superlayer is a much better match to the granularity required at small radius than a wire based tracking system (Figure 6).

The primary job of the IFT will be offline track pattern recognition, but it also provides a fast level 1 tracking trigger.

CTC replacement

With future Tevatron luminosity improvements, as the luminosity increases beyond $10^{32} \text{cm}^{-2} \text{sec}^{-1}$, even the outer layers of the CTC will have un-

be removed for Run II. This space can then be used for the fiber tracker.

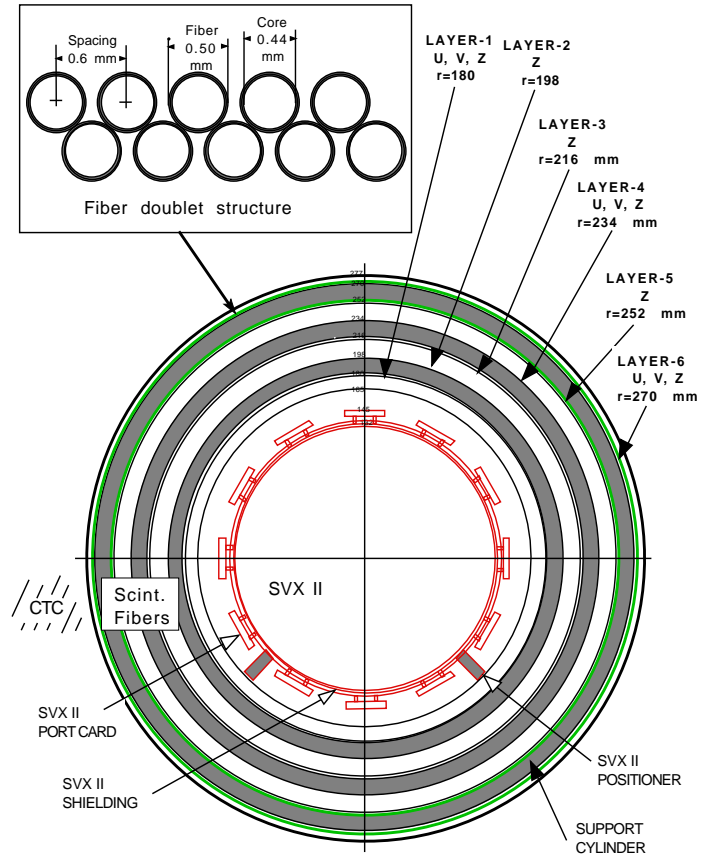


FIG. 5. The Intermediate Fiber Tracker (IFT).

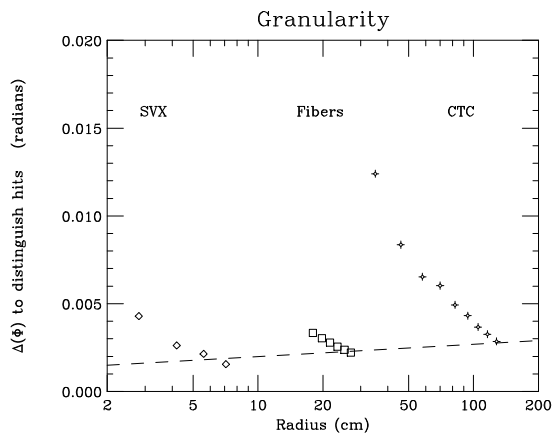


FIG. 6. Comparison of the azimuthal angle granularity of the tracking subsystems. A rough ‘two-track angular resolution’ is calculated by taking *a*) two times the axial strip width divided by the radius for the SVX, *b*) 600 microns (the singlet fiber spacing) divided by the radius for the fibers, *c*) the average pulse width divided by the radius for the CTC. The dashed line is meant to set the scale in a dense jet tracking environment; 10% of the time, there will be a second track less than that distance from a high P_t track in top events.

acceptable occupancy. Currently, bunch crossings happen every 3.5 microseconds, and there are 3 minimum bias interactions per crossing at $0.2 \times 10^{32} \text{cm}^{-2} \text{sec}^{-1}$. For Run II the time between bunches will be reduced initially to 396 ns (corresponding to 3 minimum bias interactions per crossing at $10^{32} \text{cm}^{-2} \text{sec}^{-1}$), and then to 132 ns (corresponding to 3 minimum bias interactions per crossing at $3 \times 10^{32} \text{cm}^{-2} \text{sec}^{-1}$). Thus occupancy in the SVX II and IFT can be kept to a reasonable level by increasing the number of bunches, keeping the luminosity per bunch crossing low. However, this strategy does not help the CTC because of its 800 ns drift time. For luminosity above $10^{32} \text{cm}^{-2} \text{sec}^{-1}$, the CTC should be replaced with a device with < 100 ns drift time.

CDF is currently examining two technologies for the CTC replacement chamber. A CTC style chamber with twice the drift velocity and cells one fourth the size of the CTC is one option. An SDC style straw chamber is the other option.

Time of Flight Counters

The advent of photomultiplier tubes that work well in high magnetic fields allows the installation of a simple, high precision time of flight system inside the CDF solenoid. An array of 216 scintillation counters (Figure 7) placed around the outer radius of the CTC, with time of flight resolution ~ 100 ps,

FIG. 7. TOF counter.

will resolve kaons from pions at the 2σ level over the momentum range from 0.3 GeV/c to 1.6 GeV/c. In the rapidity range $|\eta| < 1$, 55% of the kaons from B decay are in this momentum range. Hence this detector will significantly enhance the B physics program of CDF.

Scintillating Tile Calorimeter

The gas calorimeters in the end plug and forward regions of CDF will be replaced with one new scintillation counter based calorimeter. The new system will result in increased compactness, hermiticity, radiation hardness, and speed.

The scintillating tiles are arranged in a projective tower geometry. The light is collected with wavelength shifting fibers connected to clear fibers, which are read out with photomultiplier tubes (Figure 8). The electromagnetic section uses lead absorber, and the hadronic section uses iron absorber. The expected EM energy resolution is $\sigma/E = 17\%/\sqrt{E} \oplus 1\%$, and the expected hadronic energy resolution is $\sigma/E = 80\%/\sqrt{E} \oplus 5\%$, where E is in GeV.

At a depth of six radiation lengths inside the EM calorimeter is a shower max detector consisting of two crossed layers of scintillator strips read out with multi-anode phototubes. The position resolution is expected to be about 1.5 mm for 10 GeV electrons.

Muon Chambers

Large sections of the Central Muon Upgrade (CMP) and Central Muon Extension (CMX) were actually in place for Run I (Figure 1). The CMP coverage of 70% of the barrel will be increased to 84% for Run II, and the current CMX coverage of 66% of ϕ will be increased to 93%.

Moving the forward muon toroid system (FMU) closer to the central detector (Figure 1) will change its coverage from $2.0 < \eta < 3.6$ to $1.5 < \eta < 3.0$. This will increase the FMU acceptance for muons from W decays by a factor of 1.5, and the FMU $Z \rightarrow \mu\mu$ acceptance by a factor of 1.8. The $1.5 < \eta < 2.0$ region of the FMU will also benefit from the SVX II + IFT tracking capability in that region.

FIG. 8. The CDF tile-fiber upgrade calorimeter, which replaces the current plug and forward gas calorimeters.

Electronics, DAQ and Trigger

The change in Tevatron operating conditions from 3.5 microsecond bunch spacing and luminosity of $2 \times 10^{31} \text{cm}^{-2} \text{sec}^{-1}$ for Run I to 132 ns bunch spacing and luminosity of $2 \times 10^{32} \text{cm}^{-2} \text{sec}^{-1}$ for Run II necessitates almost complete replacement of the front end electronics, DAQ and trigger.

In the current scheme, a level 1 trigger halts any further data taking until a decision is made concerning an event, and if the event is accepted, data taking halts until that event is completely read out. In the Run II “deadtimeless” scheme (Figure 9), the full data from all detector elements from each crossing is kept in a 42-event-deep buffer array; events continue to be collected while the level 1 decision is made and the selected events are transferred to level 2 buffers. Events then accepted by the level 2 trigger are transferred to a level 3 trigger computer farm. Here, nearly full offline style reconstruction of the event occurs before the final decision of whether to keep the event is made. The system incurs deadtime only if all of the four level 2 buffers are full. Simulations indicate that with a 40 kHz level 1 accept rate, a 20 microsecond level 2 decision time, a 1 kHz level 2 accept rate, and a 500 microsecond event readout time, the livetime is about 90%.

The trigger will also be improved in other ways. For example, the tracking trigger information, which is currently generated at level 2, will be available at level 1 in Run II. And fast SVX track reconstruction, which is not done

FIG. 9. Trigger and data acquisition flow.

at all in the current trigger scheme, will be done at level 2, enabling triggers based on track impact parameter.

PHYSICS PROSPECTS

Of the large array of measurements that will be possible in Run II, a few are chosen here to illustrate the physics potential and demonstrate the added capabilities of the upgraded detector.

Top Mass

The current CDF measurement (1) of the top mass is $176 \pm 8 \pm 10 \text{ GeV}/c^2$. The measurement uses events with a high P_t isolated lepton plus four jets, where one of the jets has been tagged as a b -quark jet by looking for a secondary vertex using the SVX detector. Table 2 indicates how the event sample will scale to Run II.

The current statistical error of $8 \text{ GeV}/c^2$ will be reduced to $1 \text{ GeV}/c^2$ using the Run II data. If the systematic errors also all scaled as $1/\sqrt{n}$, then an overall error of $2 \text{ GeV}/c^2$ could be achieved. This scaling may well be true for several of the systematic errors, where calibration samples will grow also. For example, the calorimeter energy scale for jets can be measured by looking at events where a jet is balanced by a Z^0 or photon, and the W +jets background shape can be taken from Z +jets events. The systematic error which is hardest

TABLE 2. Yield of (lepton + 4 jet + b tag) top events for mass analysis

Currently:	19 candidates - 6.9 background	= 12 top
Improvements:	More luminosity $1 \text{ fb}^{-1} / 67 \text{ pb}^{-1}$	x 14.9
	Higher beam energy $1.8 \text{ TeV} \rightarrow 2.0 \text{ TeV}$	x 1.4
	Calorimeter+muon+tracking upgrade $ \eta_l < 1 \rightarrow \eta_l < 2 $	x 1.3
	Longer, double sided SVX II, + IFT $\epsilon_{SVXtag} = 42\% \rightarrow \epsilon_{SVX IItag} = 81\%$	x 1.9
Scaled to Run II:		= 630 top
Using theory + M.C.		570 top

to estimate at this point is the one due to gluon radiation and the top signal shape. One handle on this is to reconstruct the W mass using the jets in the top events themselves; this should allow one to measure the effect of the out-of-cone corrections. The best current estimate is that the error on the top mass will be somewhere between 3 to 5 GeV/c^2 .

One interesting thing to note is that because of the much larger acceptance of SVX tagging with the tracking upgrades in Run II, there will be approximately 290 lepton plus four jet top events in which *both* b -quark jets will be tagged. The combinatorics in the top mass fit would be much reduced by using this sample, where the jets from the b -quarks are uniquely separated from the jets from W decay.

W mass

CDF measures the W mass by fitting the transverse mass distribution of $W \rightarrow e\nu$ and $W \rightarrow \mu\nu$ events. CDF's currently published measurement (2) of $M_W = 80.41 \pm 0.18 \text{ GeV}/c^2$ was made using 19 pb^{-1} of data from Run Ia, and dominates the world average. Table 3 shows the contributions to the error estimates for each channel, and how they are expected to scale to Run II.

The control samples, such as J/ψ events to set the momentum scale and Z^0 events to measure the resolution, will grow as fast as the W event samples. Thus substantial reductions are expected for most of the systematic errors. The biggest uncertainty in Run II comes from the theoretical model, dominated by the parton distribution functions. Here, better measurement of the W asymmetry will help. It is also possible to raise the minimum transverse mass used in the fit, decreasing the dependence on the parton distribution functions at the expense of some statistical power.

Source of Uncertainty	Run Ia			Run II		
	Uncertainty (MeV/c ²)			Uncertainty (MeV/c ²)		
	$W \rightarrow e\nu$	$W \rightarrow \mu\nu$	Common	$W \rightarrow e\nu$	$W \rightarrow \mu\nu$	Common
Statistical	145	205	—	14	20	—
Lepton E , P Scale	120	50	50	20	15	15
E_e , P_μ Resolution	80	60	—	8	6	—
Recoil modeling	60	60	60	6	6	6
Trigger, Select Events	25	25	—	10	10	—
Backgrounds	10	25	—	5	10	—
Theoretical Model	75	75	65	30	30	30
Fitting	10	10	—	5	5	—
Total Uncertainty	230	240	100	42	40	34
e and μ Combined	180			38		

TABLE 3. Summary of uncertainties in the Run Ia W mass measurement, and the extrapolation to 2 fb⁻¹ of data in Run II.

Indirect measurement of Higgs mass

In the minimal standard model, the top mass, W mass, and Higgs mass are related as shown in Figure 10. The fact that the point representing the CDF measurements of top mass and W mass lies on the Higgs band is a significant affirmation of the standard model. With the more precise measurements in Run II, this will turn into an indirect measurement of the Higgs mass, as also indicated in Figure 10.

BF($t \rightarrow Wb$)

The large number of top events which will be available in Run II will allow CDF to do more detailed top physics than just the mass and cross section. For example, by taking the number of $t\bar{t}$ event candidates with one b -quark tagged jet and the number with two b -quark tagged jets, and using the expected efficiencies, CDF can measure the fraction of the time that t decays to b plus a W , versus any other quark q . The current preliminary CDF measurement using 67 pb⁻¹ of data is

$$\frac{Br(t \rightarrow Wb)}{Br(t \rightarrow Wq)} = 0.87^{+0.13+0.13}_{-0.30-0.11}$$

The extended coverage of the SVX II detector upgrade will significantly aid this measurement, by doubling the efficiency of tagging jets. With 2 fb⁻¹

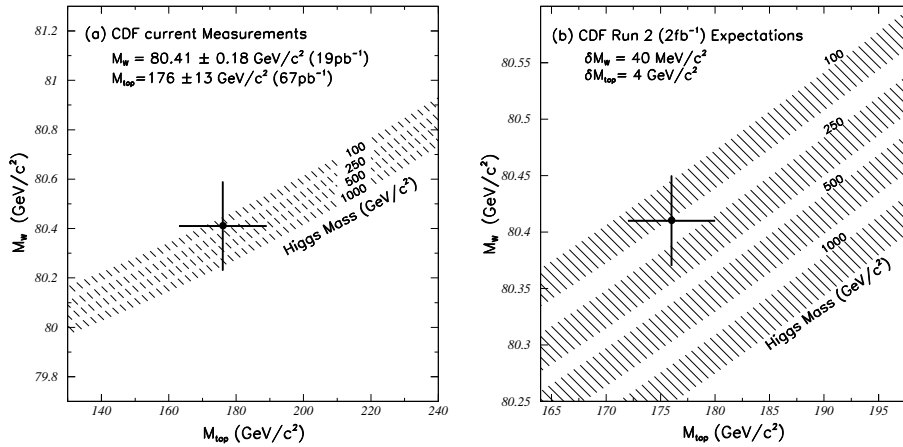


FIG. 10. The data point in the left figure is the CDF measurement of M_W and M_{top} , and the point in the right figure represents the CDF error estimate for 2 fb^{-1} of data. The curves are from a calculation (3) of the dependence of M_W on M_{top} in the minimal standard model using several Higgs masses. The bands are the uncertainties obtained by folding in quadrature uncertainties on $\alpha(M_Z^2)$, M_Z , and $\alpha_s(M_Z^2)$.

of data in Run II, it is expected that the error on this measurement will be reduced to 3%.

CP Asymmetry in $B \rightarrow J/\psi K_s^0$

The only currently measurable CP asymmetry is in the Kaon system. However, measurable asymmetry is predicted in the B_d system. Specifically, the asymmetry between the decay rates of $B^0 \rightarrow J/\psi K_s^0$ and $\overline{B}^0 \rightarrow J/\psi K_s^0$ is a measure of the “unitarity triangle” angle β . The ability to do this measurement depends both on reconstructing the B meson, and on flavor tagging it as a B^0 or \overline{B}^0 by using other information in the event.

CDF has collected a sample of reconstructed $B^0 \rightarrow J/\psi K_s^0$ events, where $J/\psi \rightarrow \mu^+ \mu^-$, in the current Run I data (Figure 11). For Run II, we plan to lower the trigger threshold for the μ^\pm from 2.5 GeV/c to 1.5 GeV/c, and use $J/\psi \rightarrow e^+ e^-$ as well. This would result in a sample of 20,000 reconstructed events for an integrated luminosity of 2 fb^{-1} in Run II. Table 4 gives a list of flavor tagging methods. As shown in the table, the dilution (which measures power of the tagging method after accounting for mistags) has been measured in CDF data samples for two of these methods; measurements are in progress for the other methods.

With 20,000 events, and using only the two measured tagging methods, the error on $\sin(2\beta)$ would be ± 0.14 . With the other tagging methods included, we expect the error on $\sin(2\beta)$ will be of order ± 0.07 .

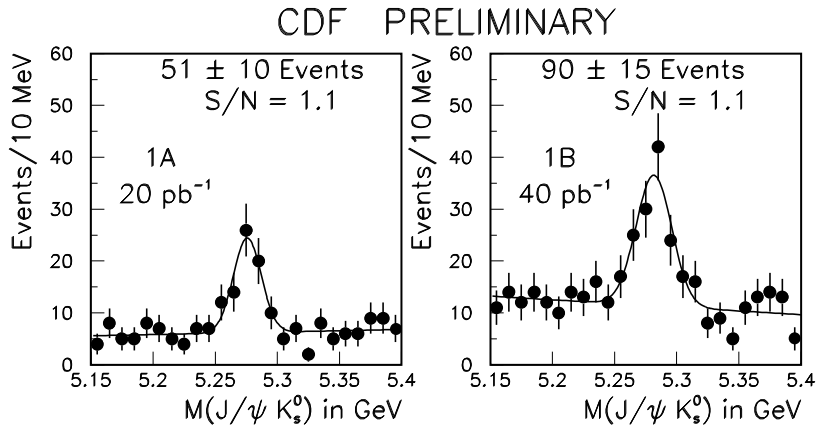


FIG. 11. Reconstructed $B \rightarrow J/\psi K_s^0$ events in CDF from Run Ia and Run Ib.

TABLE 4. Flavor tagging methods.

Flavor tagging method	Measured ϵD^2 (CDF preliminary)	Upgrades
jet charge	$1.0\% \pm 0.3\%$	
charge of central muon	$0.7\% \pm 0.2\%$	
charge of non-central muon	?	IFT, move up FMU
charge of electron	?	plug calorimeter, SVX II, IFT
charge of same side pion	?	
charge of opposite side kaon	?	TOF
vertex charge	?	SVX II

CDF also has the possibility of collecting a substantially larger data sample. The estimate above uses only central ($|\eta| < 1$) di-lepton triggers. By using the new level 2 SVX track reconstruction trigger to require a finite impact parameter, one can handle the trigger rate from triggering on a single central lepton. The use of this larger sample could lower the error on $\sin(2\beta)$ to the order of ± 0.03 .

CP Asymmetry in $B \rightarrow \pi^+ \pi^-$

The ability to measure the CP Asymmetry in $B \rightarrow \pi^+ \pi^-$, which is a measure of the unitarity triangle angle α , depends heavily on many of the detector upgrades.

The current CDF track trigger operates at trigger level 2. Since this final state does not include any leptons or a distinctive calorimeter signature, we cannot currently trigger on this decay mode at trigger level 1. The Run II

upgrade of moving the tracking trigger to level 1 will allow us to trigger on this state by requiring two tracks, each with $P_t > 2 \text{ GeV}/c$.

The current bandwidth of CDF at level 1 would also be inadequate, but the implementation of the “deadtimeless DAQ” will allow us to take the expected rate of 17 kHz at a luminosity of $10^{32} \text{ cm}^{-2} \text{ sec}^{-1}$.

Requiring a finite secondary vertex decay distance with the new SVX trigger keeps the rate at level 2 down to an acceptable 20 Hz.

The measurement will also benefit from the improved flavor tagging abilities mentioned in the previous section.

An additional complication comes from other B backgrounds. The backgrounds due to $B_d \rightarrow K^+ \pi^-$ and $B_s \rightarrow \pi^+ K^-$, which produce mass peaks $40 \text{ MeV}/c^2$ away from the $B \rightarrow \pi^+ \pi^-$ peak can be handled because of the excellent mass resolution of the CTC, which is estimated to be about $28 \text{ MeV}/c^2$ for Run II conditions. The dE/dx system of the CTC allows one to statistically separate out $B_s \rightarrow K^+ K^-$ events, which otherwise constitute an irreducible background under the $B_d \rightarrow \pi^+ \pi^-$ peak.

The expected error on $\sin(2\alpha)$ is ± 0.14 with 2 fb^{-1} of data in Run II.

SUMMARY

The CDF detectors, front end electronics, DAQ, and trigger are being upgraded to handle the higher luminosity expected in Tevatron Run II. In addition, several capabilities are being added: higher quality calorimetry in the end plug region, tracking in the region $1 < \eta < 2$, the ability to measure track impact parameter in the $r - z$ plane with the SVX II, the ability to trigger on SVX II $r - \phi$ impact parameter, and a time-of-flight system. There is an exciting range of physics that will be accessible with this upgraded detector, and the large data sets that the higher Tevatron luminosity will provide.

REFERENCES

1. F. Abe *et al.*, Phys. Rev. Lett. **74**, 2626 (1995).
2. F. Abe *et al.*, Measurement of the W boson mass, FERMILAB-PUB-95-035-E (1995), submitted to Phys. Rev. Lett.
3. The curves are calculated using a FORTRAN program from F. Halzen and B.A. Kniehl (private communication), described in Nucl. Phys. **B353**, 567 (1990).